Analyze SST within the NCEP GFS, Part I: 3DVAR GSI

Xu Li, John Derber, Shrinivas Moorthi, Andrew Collard

IMSG at NOAA

Environment Modeling Center, National Center for Environmental Prediction

KEY WORDS: Sea Surface Temperature (SST), Near-Surface Sea Temperature (NSST), direct assimilation, Numerical Weather Prediction (NWP)

Abstract

The SST, with the foundation temperature as the analysis variable, has been analyzed together with the atmospheric analysis variables within the NCEP GFS with 3DVAR GSI.

The concept of the SST has been extended to the Near Sea Surface Temperature (NSST) profile due to diurnal warming and sub-layer cooling physics. All the observations, including satellite radiances and in situ sea water temperature, are assimilated directly with the observation operators and their Jacobians provided by a Radiative Transfer Model and NSST model.

The NSST model consist of a Diurnal Thermocline Layer model, DTL-1p, which is developed based on Price-Weller-Pinkel one-dimensional model, and a Thermal Skin Layer model or parameterization adopted from Fairall. The NSSTM is built in the atmospheric forecasting model and integrated forward with the same time step.

The results shows the SST has been improved in both analysis and prediction mode. The new SST analysis has positive in the use of the surface sensitive satellite radiances as well. The impact on the weather forecasting is positive in tropics and neutral in higher latitude areas.

1. Introduction

Since no oceanic model included yet in the current Numerical Weather Prediction (NWP), Sea Surface Temperature (SST) is the only oceanic variable needed and therefore the oceanic component means SST only. Under this circumstance, the prediction is made by an integrated system of an atmospheric numerical model and an atmospheric data assimilation system, such as the NCEP (National Center for Environmental Prediction) GFS (Global Forecast System). SST is prescribed as the combination of the analyzed initial SST anomaly and the SST climatology with seasonal variability in the prediction mode.

The slow evolving ocean is the basis to handle the ocean in the simple way in NWP. Indeed, the evaluation of the prescribed SST prediction in the NCEP GFS has shown the area average error grows very slow and maintains a few tenth degrees up to 7 days in the prediction mode (see session 4 of this

paper), which is a few times smaller than that for the air temperature. The advantage of the coupled atmosphere-ocean model can be achieved only if the predicted SST has even smaller errors, even if it does provide more realistic interaction at the interface.

There are two SST analysis have been used in the operational NCEP GFS, one is a $1^{\circ} by\ 1^{\circ}$ weekly SST analysis, which is analyzed daily but with the observations in a 7-day time window (Reynolds et al, 1994) and the other one is daily Real-Time Global (RTG) SST (Thiébaux et al, 2003) with the higher resolution ($\frac{1}{12^{\circ}}$) . They are referred as Reynolds SST and RTG SST analysis respectively.

The Reynolds weekly SST analysis had been used by NCEP and other NWP operational centers for many years. The low resolution SST analysis is fine due to the slow varying fact and, in the early period, the observation coverage could not support higher resolution analysis. At present, a few more SST analysis products are available over the world and are analyzed daily with the increasingly improved observation network, particularly the satellite one. The precision of these SST analysis products is reported to be around 0.5 K. In fact, it is just for the global scale and can be much larger for the smaller spatial and temporal scale. In 2002 GODAE (Global Ocean Data Assimilation Experiments), recognizing that none of the SST measurements available could meet the precision specification of 0.4 K to make oceanic prediction operationally, the GODAE High-Resolution SST Pilot project (GHRSST-PP) was initiated (Donlon et al, 2007).

As a representative of GHRSST-PP, OSTIA (Operational Sea Surface Temperature and Sea Ice Analysis) has made some progresses in SST analysis, such as the inclusion of diurnal warming and sub-layer cooling effects, the use of multi satellites and the uncertainty estimate of various retrieval products (Donlon et al, 2012). A new variable, the foundation temperature, T_f T_f , is introduced to address the vertical thermal structure in the upper most layer of the ocean. The strategy is to provide T_f T_f analysis and let users obtain the SST by themselves with the diurnal warming and sub-layer cooling model. Since Optimum Interpolation (OI) is adopted as the analysis scheme, all the observations need to be converted to the analysis variable, foundation temperature. In principle, both diurnal warming and sub-layer cooling models are required for this conversion. However, in OSTIA, a warming model is not applied since only the observations to represent the foundation temperature are used by removing the data with large warming signal, based on the wind speed and insolation, and a simplified sub-layer cooling parameterization is applied to convert the retrieved skin temperature into foundation temperature. The analysis is performed every 24 hours. The validation has indicated this product has zero bias and 0.57 K RMS.

SST acts as the lower boundary condition of both the atmospheric model and radiative transfer model (RTM), which is another important component of the modern NWP for assimilating the satellite data directly and therefore more effectively. At the forecasting step, SST is critical to the flux calculation at the air-sea interface and therefore to the prediction and the background quality for the analysis. The significance of the SST impact on the fluxes depends on the meteorological conditions. Webster et al (1996) showed that the change in surface heat flux components associated with a 1.0 degree change in SST for average conditions during the TOGA COARE IOP is 6.3, 2.4 and 18.3 w/m^2 for upwelling longwave, sensible and latent heat flux respectively. In proportion, they correspond to the flux change by

1.3%, 23.3% and 16.7% respectively. At the analysis step, high quality SST is required to simulate the background equivalent of the satellite radiance accurately by a RTM with the atmospheric profile and underlying surface condition. For surface sensitive channels, the sensitivity of the satellite brightness temperature to SST is usually in the range of 0.2 to 1.0. Very often, the impact of the SST, through error in the simulated radiance due to SST analysis, on the evaluation of the innovation, the departure of the observed radiance from the background, and the implementation of the data quality control is significant.

The reduction of the SST analysis error can improve not only model performance but also its initial conditions quality. The error sources include the limited observations, the use of the observations, particularly the extraction of thermal signal from the satellite radiances, the background and observation error covariance, the inclusion of the high frequency SST variability, such as diurnal warming and skin layer cooling, and related vertical structure, the analysis algorithm and so on.

In this paper, the improvement is achieved by resolving vertical and the high frequency variability near the sea surface due to diurnal warming and sub-layer cooling, clarifying the analysis variable, using more observations and assimilating the observations directly with the NCEP GFS.

The general picture of the vertical temperature structure, downward from the surface, is mixed layer, seasonal thermocline and then deeper ocean. The existence of the mixed layer affects the work related to SST profoundly. It permits the integration of the control equations along vertical direction and simplifies the problem in oceanic modeling and turbulence mixing study. It allows the lower vertical resolution near the sea surface for an Oceanic General Circulation Model (OGCM). It makes it easier to use a various types of observations in the analysis of the upper ocean since they can be used depth independently. However, just below the sea surface and, usually, above the base of the mixed layer, there exist a Thermal Skin Layer (TSL) and a Diurnal Thermocline Layer (DTL), corresponds to the sub-layer cooling and diurnal warming events respectively (Robinson, 2005). The cooling amount across the TSL is about $0.2\,K$ in average and can be up to $1.0\,K$, The diurnal warming amount across DTL can be up to 5 to 6 degree (Gentemann et al, 2008). Diurnal warming event is active for hours per day and in a limited region when the conditions satisfied, the conditions to support the sub-layer cooling effect are satisfied much more easily. Therefore, the cooling effect dominates in the large area mean of these two amounts.
With the existence of TSL and DTL, a few terms, SST_{int}, SST_{skin}, $SST_{subskin}$, SST_{depth}, and SST_{fnd} are introduced to represent the temperatures in DTL (Donlon et al, 2007). SST_{int} is the temperature at the air-sea interface ($z = 0$) and not observed directly by any instrument. SST_{skin} is the temperature at the depth of about $20\,\mu m$ and observed by Infra-Red instruments with $11\ to\ 12\,\mu m$ wavelength. $SST_{subskin}$ is the temperature with the depth in the order of $1\,mm$ and observed by Microwave instruments with $6\ to\ 11\,GHz$ frequency. SST_{depth} is the temperature at the depth in the range of $20\,cm\ to\ 5\,m+$ and observed by the buoys and ships. SST_{fnd} is the temperature at the base of DTL, with the order of $(5m)$ and is location dependent, the stronger the warming event, the shallower the DTL, and can be observed directly by some in situ instruments. These new SST terms help to understand what is observed and analyzed and also lead to the foundation temperature becomes an analysis variable in modern SST analysis.

Actually, these SSTs are just feature temperatures or a subset of a T-Profile $T(z)$. They are not independent but related. A new term, Near Surface Sea Temperature (NSST) is introduced here to represent the vertical structure due to DTL and TSL. If an NSST Model (NSSTM) is available to simulate the T-Profile and also provide the observation operator and its Jacobian for a variational assimilation, the analysis variable doesn't have to be observed directly.

The diurnal cycle of the ocean has drawn more and more attention in the weather and climate community. A few diurnal warming models are available and have been applied to improve the air-sea interface heat fluxes, resolve the SST diurnal variability in NWP and the simulation of the diurnal warming profile successfully (Fairall et al, 1996, Zeng et al, 2005 and Gentmann et al, 2009). Fairall's model is based on a scale analysis version of the Price-Weller-Pinkel (PWP) model (Price et al, 1986), the DTL thickness is specified to be 3 meters in Zeng's model since only the temperature equation is used, and the free convection adjustment due to the static stability is not included in all these models. The goal here is not only the NSST-Profile simulation, but also the required Jacobian (the sensitivity among the temperature at different depth in the DTL layer) to assimilate the depth dependent observations directly, a new DTL model has been developed, referred to NCEP DTM-1p. This model is based on the primitive PWP model and therefore more complete physics, including the inclusion of the fresh water flux, earth rotation effect, the sensible heat flux due to the precipitation. The free convection adjustment has been addressed to help the more natural decay and then the end of the established warming event. And the Jacobian for the temperatures in the DTL has been developed as well.

A well-defined analysis variable is the starting point of any analysis, since every element of the analysis scheme is based on this definition, including the observation and simulation of this variable, the evaluation of the innovation, the observation and background error and so on.

Historically, the bulk temperature (T_{bulk}) has been the analysis variable in the SST analysis. T_{bulk} is defined as the upper mixed layer temperature. However the term tends to be applied loosely to the temperature measured by buoys or ships. This is not a problem when there is a mixed layer without the vertical structure. With the effort to address the sub-layer cooling and diurnal warming effects, which corresponds to Thermal Skin Layer (TSL) and Diurnal Thermocline Layer respectively (Robison, 2005), foundation temperature (T_f) started to be used as the analysis variable in some SST analysis (Donlon et al, 2007; Donlon et al, 2012). T_f is the temperature at the base of DTL Physically but loosely, both T_{bulk} and T_f are the mixed layer temperature (T_{mix}), since $T_{bulk} = T_{mix}$ and $T_f = T(z = z_w) = T_{mix}$, when the DTL thickness (z_w) is smaller than the mixed layer depth, which is usually true.

If the observations are treated as time and depth independent, as done in the current daily analysis schemes, there is an inconsistency between the observation and the analysis variable. Since the observations are depth dependent and instantaneous in a 24-hour time window, but the analysis variable is re-defined to be the 24-hour mean mixed layer temperature, for T_{bulk} analysis variable case, or the temperature at the depth of DTL base and early morning time just before the onset of DTL, for T_f analysis variable case. Obviously, this inconsistency is a problem when the time evolution and vertical

structure need to be addressed in SST analysis. This problem is alleviated in some T_f analysis by tossing the observations with diurnal warming signal.

Both T_{bulk} and T_f are sea water temperature, however, it is indirectly observed by the satellite instruments in the form of radiance. In order to be able to compare the indirect observation (radiance) and the first guess or background (temperature) of the analysis variable, and then get the innovation which is the difference between the observation and background, there must be a way to relate the radiance and temperature. The first way, referred to retrieval, is to retrieve the temperature from the radiance and then innovation is available in the form of temperature. The second way, referred to direct assimilation, is to relate or convert the water temperature background to the radiance, with a RTM and atmospheric profile of temperature, humidity and other parameters, and then the innovation is available in the form of radiance. The retrieval method is used in all the current SST analysis. The direct assimilation has been used in major NWP operational centers in their atmospheric data assimilation system since late 1990's. Direct assimilation of the radiance uses the satellite data more effectively by exacting the information from the satellite observation more optimally with the variational assimilation technique, but not used in SST analysis yet. The most important advantage of the direct assimilation over retrieval is the determination of the observation covariance. The observation error covariance is complicated and therefore difficult to be specified for the SST retrieval, which is used as the observation in analysis. But in direct radiance assimilation, the radiance observation can be treated as diagonal with good confidence. Another problem of the SST retrieval is the uncertainty in the depth of the retrieved temperature. The retrieval depth depends on the retrieval algorithm or what the retrieved SST is tuned to, the buoy or other in situ data. This can overcome in the direct assimilation while the wavelength or frequency dependent temperature can be provided to RTM.

Here, the SST, with T_f as the analysis variable, is analyzed 6-hourly within the NCEP GFS with 3DVAR GSI. All the observations are assimilated directly with the Community Radiative Transfer Model (CRTM) and the NSSTM.

The NSST model is described in section 2, including the derivation of the DTL model, the adoption of a TSL parameterization scheme, observation operator and its Jacobian required to analyze T_f within the NCEP GFS. Section 3 discuss how T_f, an oceanic variable, is analyzed in the NCEP GFS. The result and analysis is in section 4.

2. **Near Surface Sea Temperature T-Profile simulation**

The NSST-Profile is assumed to be linear and therefore the layer thickness and the cooling/warming amount at the surface determine the whole profile.

2.1 Thermal Skin Layer (TSL) Model

The parameterization by Fairall et al (1996) is adopted to get TSL thickness, δ_c, and the cooling amount at the surface, $T_c'(0)$.

$$\delta_c = C_1\{1 + [C_2(Q - S_c + C_3H_l)]^{3/4}\}^{-1/3} \quad (1)$$

$$T_c'(0) = \delta_c(Q - S_c)/\kappa \quad (2)$$

Here, $C_1 = \frac{6\upsilon}{\kappa(\frac{\rho_a}{\rho})^{1/2}u_{*a}}$, $C_2 = \frac{16g\alpha\rho c_p\nu^3}{u_{*a}^4(\frac{\rho_a}{\rho})^2\kappa^2}$, $C_3 = \frac{S\beta c_p}{\alpha L_\nu}$, $Q = H_s + H_l + Q_{rain} - R_{nl}$, κ is the thermal conductivity of the water, ρ_a is the air density, ρ_a is the water density, u_{*a} is the atmospheric friction velocity, υ is the kinematic viscosity, $L_v = (2.501 - 0.00237T_s)\times 10^6$, is the vaporization latent heat at the surface temperature T_s, α *and* β is the thermal expansion coefficient and saline contraction coefficient respectively, c_p is the specific heat of the water, Q is the non-solar heat flux, H_s is the sensible heat flux, H_l is the latent heat flux, Q_{rain} is the sensible heat flux due the difference of the water and rainfall temperature, R_{nl} is the net long wave radiation, all the fluxes are positive upward.

$H_b = Q - S_c + C_3H_l$ the virtual surface cooling that includes the buoyancy effects of salinity due to evaporation.

$f_c = a_1 + a_2\delta_c - (a_3/\delta_c)(1 - e^{-\delta_c/a_4})$, Where $a_1 = 0.137$, $a_2 = 11$, $a_3 = 6.6\times 10^{-5}$, $a_4 = 8\times 10^{-4}$

$S_c = f_c(\delta_c)R_{ns}$ is the amount of the solar radiation absorbed in TSL.

Assume a linear profile in TSL, then

$$T(z) = (1 - \frac{z}{\delta_c})T_c'(0), \quad 0 < z \leq \delta_c \quad (3)$$

2.2 Diurnal Thermocline Layer (DTL) Model

2.2.1 Brief introduction to Price-Weller-Pinkel one-dimensional model

The DTL model is based on the Price-Weller-Pinkel (PWP) model (Price et al, 1986), assuming the diurnal cycle rides passively and non-interactively on top of the ambient oceanic variability. Then, the control equations for the DTL diurnal cycle amount, including the temperature, salinity, zonal and meridonal currents are the usual one-dimensional form:

$$\frac{\partial T'}{\partial t} = -\frac{1}{\rho_0 c_p}\frac{\partial F}{\partial z} - \frac{1}{\rho_0 c_p}\frac{\partial I}{\partial z} \quad (4)$$

$$\frac{\partial S'}{\partial t} = -\frac{\partial M}{\partial z} \quad (5)$$

$$\frac{\partial u'}{\partial t} - fv' = -\frac{1}{\rho_0}\frac{\partial \tau_x}{\partial z} \quad (6)$$

$$\frac{\partial v'}{\partial t} + fu' = -\frac{1}{\rho_0}\frac{\partial \tau_y}{\partial z} \quad (7)$$

Here, ρ_0 is the reference water density, $F(0) = Q = H_s + H_l + Q_{rain} + R_{nl}$ is the non-solar heat flux at the air-sea interface, H_s, H_l, Q_{rain}, R_{nl} are the same as in 2.1. $M(0) = S_r(E - P)$ is the freshwater flux times surface salinity; τ_x, τ_y is the wind stress in x and y direction. $I(z)$ is the solar radiation penetrating the sea water, positive downward. The parameterization of solar absorption follows

a 9-band spectral scheme (Paulson and Simpson, 1981; Gentemann et al, 2009) and the subsurface solar angle effect is not included.

Define thermal expansion coefficient as: $\alpha = -(\frac{d\rho}{dT})/\rho_0$, saline contraction coefficient as: $\beta = -(\frac{d\rho}{dS})/\rho_0$. Both α and β have positive value. Therefore, the density change due to the DTL is $\Delta\rho = -\alpha\rho_0\Delta T + \beta\rho_0\Delta S$. Here, ΔT is always greater zero, but ΔS depends on the sign of $E - P$.

In PWP model, the vertical mixing is realized by adjusting the profile available at the time with three criteria and there is no mixing term explicitly in control equations. This requires very high vertical resolution. The three criteria are: (1) Static stability $(\partial\rho/\partial z \geq 0)$; (2) Mixed layer stability $(\frac{g\Delta\rho h}{\rho_0(\Delta V)^2} \geq 0.65)$; (3) Shear flow stability $(\frac{g\partial\rho/\partial z}{\rho_0(\partial V/\partial z)^2} \geq 0.25)$.

The insight into the mixing or the profile adjustment based on the three criteria is critical (Niiler PP, and Kraus EB. 1977).

2.2.2 The derivation of DTL model

Let z_w represent the DTL thickness, assume the vertical profile of the DTL temperature, salinity, zonal and meridional currents is linear in the range of 0 to z_w, and C_h, C_s, C_u *and* C_v as follows for a more compact form of the DTL model equations, particularly for the DTL thickness control equation.

$C_x = \int_0^{z_w} x'(z,t)dz = \frac{1}{2}x'(0,t)z_w$, x can be T, S, u *or* v.

The value of C_x equals to the area of a right triangle with $x'(0,t)$ and z_w as its two sides, and can be understood as the content in DTL, for example, C_t is the heat content. The DTL control equations as follows:

$$\frac{\partial C_t}{\partial t} = \frac{1}{\rho_0 c_p}[f_w(z_w)I_0 - Q] \tag{8}$$

$$\frac{\partial C_s}{\partial t} = S_r(E - P) \tag{9}$$

$$\frac{\partial C_u}{\partial t} = fC_v + \frac{\tau_x}{\rho_0} \tag{10}$$

$$\frac{\partial C_v}{\partial t} = -fC_u + \frac{\tau_y}{\rho_0} \tag{11}$$

$$\frac{\partial z_w}{\partial t} = (\frac{\tau_x C_u + \tau_y C_v}{\rho_0} + \frac{g}{4R_{ic}}z_w^2\Delta\rho)\frac{z_w}{C_u^2 + C_v^2} \tag{12}$$

Here,

$$\Delta\rho = -\frac{\alpha[f_w(z_w)I_0 - Q]}{c_p\rho_0} + \beta S_r(E - P)$$

Equations (5) to (8) result from the vertical integration from 0 to z_w of (1) to (4), they are not closed since the newly introduced 5th variable z_w, the DTL thickness. (9) is derived as follows to close the control equations of DTL.

For the warm layer with z_w thickness, the bulk Richardson number (R_b):

$$R_b = \frac{g(\alpha T_s' - \beta S_s')z_w}{u_s'^2 + v_s'^2} = \frac{g(\alpha C_t - \beta C_s)z_w^2}{2(C_u^2 + C_v^2)} \quad (13)$$

Apply the mixed layer stability criterion.

$$\frac{g(\alpha C_t - \beta C_s)z_w^2}{2(C_u^2 + C_v^2)} = R_{ic} = 0.65 \quad (14)$$

$\alpha \times (5) - \beta \times (6)$, gives:

$$\frac{\partial(\alpha C_t - \beta C_s)}{\partial t} = \frac{\alpha}{\rho_0 c_p}[f_w(z_w)I_0 - Q] + \beta S_r(E - P) \quad (15)$$

$C_u \times (7) - C_v \times (8)$, gives:

$$C_u \frac{\partial C_u}{\partial t} + C_v \frac{\partial C_v}{\partial t} = \frac{\tau_x C_u + \tau_y C_v}{\rho_0} \quad (16)$$

Apply $\partial/\partial t$ to (13) and then using substitutes of (14) and (15), the (9), the z_w control equation, is derived. The shear flow stability criterion cannot be applied here since the linear profile assumption.

The system with 7 ordinary differential equations is solved by integrating forward with modified Euler scheme with the same time step of the GFS atmospheric model, where the DTL model is built in.

2.2.3 Initial condition determination

The diurnal warming event occurs when certain conditions are satisfied. When DTL doesn't exist, all the control variables are zero except for $z_w = 30\ m$, let this refer to zero state. That means even the DTL model is running forward every time step, the control variables are updated only for the grids where the DTL has established, otherwise, it keeps as zero state.

For a grid with zero state, the absorbed heat in a layer just below the surface with the thickness of $z_{w\_ini} = 0.2\ m$ is judged every time step, if it is greater than zero, i.e., $f_w(z_{w\_ini})I_0 - Q > 0$, then the criterion of the onset of DTL is satisfied and the system is integrated forward to get the DTL evolution.

Let t_0 and t_1 be the start and end time of the first time step interval $\Delta t = t_1 - t_0$. Naturally, the initial conditions are the zero state except for replace z_w from z_{w_max} *to* z_{w_ini}, however, a better z_w can be derived in the same way as Fairall (1996), where the time integral is from the onset time to the current time, of wind stress and net heat flux are used. Here, the time integral is for the first time step, t_0 to t_1. Notice that the Fredholm solution (Phillips, 1977) is applied to obtain the currents in the first time step. And the currents and therefore DTL thickness rotation effect or Coriolis dependent is accounted for.

When $f \approx 0$ $(-1^\circ < latitude < 1^\circ)$, then,

$$C_u = \frac{\Delta t \tau_x}{\rho_0}$$

$$C_v = \frac{\Delta t \tau_y}{\rho_0}$$

$$z_w = (2R_{ic}\Delta t/\rho_0)^{1/2}\tau/\{(\alpha g/c_p)[f_w(z_w)I_0 - Q] - \beta g \rho_0 S_r(E-P)\}^{1/2} \quad (17)$$

When $f > 0$ $(latitude > 1^\circ)$, then,

$$C_u = \frac{\tau sin\,(f\Delta t)}{(\rho_0 f)}$$

$$C_v = -\frac{\tau[1-cos\,(f\Delta t)\,]}{(\rho_0 f)}$$

$$z_w = (\frac{2R_{ic}}{\rho_0})^{1/2}\{\frac{[2-2cos\,(f\Delta t)\,]}{(f^2\Delta t)}\}^{1/2}\tau/\{(\alpha g/c_p)[f_w(z_w)I_0 - Q] - \beta g \rho_0 S_r(E-P)\}^{1/2} \quad (18)$$

Notice, z_w is solved iteratively with $z_w^{(0)} = z_{w\_ini}$. Starting from 2nd time step: $t = t_k$, $k = 2, 3, \ldots, N$, the system go head by integrating forward.

2.2.4 The free convection adjustment

For static stability, it seems unnecessary to apply since the linear temperature and salinity profile guarantees $\partial\rho/\partial z \geq 0$, in fact, the free convection still can happen when the time dimension considered. The diagram in Figure.1 shows how the free convection adjustment is done if needed. With the known convection layer thickness (C), the DTL profile is adjusted to get a smaller warming amount at the surface $(T_w^{'(0)} \rightarrow T_w^{'})$ and a deeper warm layer base $(z_w^{(0)} \rightarrow z_w)$. $T_w^{'}$ is first determined as the average of the warming amount at $z = 0$ *and* $z = C$, corresponding to the mixing by free convection, then the warm layer thickness is adjusted to keep the heat content unchanged, in terms of geometry, the area of triangle $Oz_w T_w^{'}$ and $Oz_w^{(0)} T_w^{'(0)}$ is identical. Note the mixed layer from the surface down to free convection depth C is not kept due the linear profile convention here.

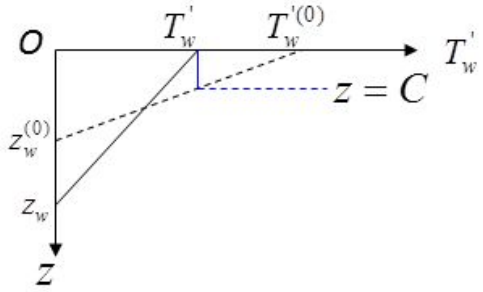

Figure 1. The diagram to implement the free convection adjustment.

The absorbed solar radiation in the layer from the surface down to depth z,

$$I_{abs}(z) = I(0) - I(z) = f_w(z)I(0) = [1 - \sum_{i=1}^{N} F_i e^{-\frac{z}{\gamma_i}}]I(0)$$

Therefore,

$$I(z) = I(0) \sum_{i=1}^{N} F_i e^{-\frac{z}{\gamma_i}}$$

The solar radiation absorption at a specific depth z : $\frac{\partial I(z)}{\partial z} = -I(0) \sum_{i=1}^{N} (\frac{F_i}{\gamma_i}) e^{-\frac{z}{\gamma_i}}$

At time , the linear sea water density profile of the DTL is

$$\rho(z) = -\alpha\rho_0(1 - \frac{z}{z_w})T'(0,t) + \beta\rho_0(1 - (1 - \frac{z}{z_w})S'(0,t) \qquad (19)$$

Assume there exist a free convection layer just below the sea surface with the thickness of C , integrate (16) from *0* to C , gives the average density in this layer:

$$\bar{\rho}(t) = (1 - \frac{1}{2z_w(t)})[-\alpha\rho_0 T'(0,t) + \beta\rho_0 S'(0,t)] \qquad (20)$$

This layer average density change due to heat and fresh water flux at this time step is

$$\Delta\bar{\rho}(t) = \frac{-[f_w(C)I(0) - Q(t)]\alpha\rho_0\Delta t}{(\rho_0 c_p) + \rho_0\beta S_r}[E(t) - P(t)]\Delta t \qquad (21)$$

At the same time, at the base of the free convection layer, $z = C$,

$$\rho(C,t) = -\alpha\rho_0 T'(C,t) + \beta\rho_0 S'(C,t) \qquad (22)$$

Its change due to heat and fresh water flux at this time step:

$$\Delta\rho(C,t) = -\frac{\alpha}{c_p}\frac{\partial I}{\partial z}|_{z=C} \qquad (23)$$

Since,

$$\overline{\rho(t)} + \Delta\bar{\rho}(t) = \rho(C,t) + \Delta\rho(C,t) \qquad (24)$$

Substitute (17), 918), (19) and (20) into (21), after some operations,

$$C = \sqrt{\frac{2z_w(t)\Delta t}{\rho_0(\alpha T'(0,t) - \beta S'(0,t))}\{\frac{\alpha}{c_p}Q(0,t) - \frac{\alpha}{c_p}[f_w(C) - sum\cdot C]I_0(t) + \beta\rho_0 S_r[E(t) - P(t)]\}}$$

Let $T'_s = T'(0,t)$, $S'_s = S'(0,t)$, and remove the time t in the equation, the derived free convection thickness can written:

$$C = \sqrt{\frac{2z_w\Delta t}{\rho_0(\alpha T'_s - \beta S'_s)}\{\frac{\alpha}{c_p}Q - \frac{\alpha}{c_p}[f_w(C) - sum\cdot C]I_0 + \beta\rho_0 S_r(E-P)\}} \quad (25)$$

Where, $m = \sum_{i=1}^{N}[(F_i/\gamma_i)e^{-\frac{C}{\gamma_i}}]$, (12) is solved iteratively, with $C^{(0)} = 0$. Obviously, there is a solution only when the expression in the radical sign is non-negative. The free convection adjustment helps the natural decay and then the end of a warming event. It is applied every time step after the system integration update is done.

2.2.4 A validation of the DTM-1p

A comparison of the diurnal warming amount ($T'^{(0)}_w$) at the surface is shown in Figure 2. A 40 by 31 area (5 W – 45 W, 12 N – 43 N) is selected since this amount from a few satellite retrieval are available (Gentmann, 2008). (a) and (b) is the $T'^{(0)}_w$ simulated by NCEP DTM-1p and COARE V3.0 respectively. (c) is the time series of $T'^{(0)}_w$ and the wind at the location of (14 W, 36 N). (d), (e), (f) is the difference of the SST retrieved at day and night time and can be used as the diurnal warming amount estimate by MODIS, SEVIRI and AMSR-E respectively.

From (a) and (b) of Figure 2, we can see the diurnal warming pattern is very close to each other between DTM-1p and COARE V3.0, but the amplitude in DTM-1p is closer to the retrievals in (d), (e) and (f). From (c), the diurnal warming's decay and end is more natural in DTM-1p than in COARE V3.0.

2.3 The observation operation operator and its Jacobian for direct assimilation

All the observations used to analyze SST are depth dependent. In order to assimilate the observations directly in a variational data assimilation system like GSI, the observation operator and its Jacobian to relate the observations the analysis variable are required. The T-Profile simulated by NSST model provides the observation operator, its Jacobian, which is basically the sensitivity of the temperature at a depth, referred as $T_z = T(z)$ to the foundation temperature.

The observation operator is available with the profile simulation by NSST Model:

$$T_f = T_z - T'_w(z) + T'_c(z) = T_z - (1 - \frac{z}{z_w)T'_w(0)} + (1 - \frac{z}{\delta_c)T'_c(0)} \quad (26)$$

The analysis variable, T_f, can be converted into $T_f = T_z$ with (20) as the observation operator.

In a variational data assimilation system, the Jacobian or the derivative of the observation to analysis variable is required.

For is situ data, the derivative is $\frac{\partial T_z}{\partial T_f}$.

Currently, over ocean, SST is used as the lower boundary condition of RTM, and $\frac{\partial T_b}{\partial SST}$ is available with the RTM.

When the NSST-Profile is available, the skin-depth and therefore wavelength dependent temperature can be provided to RTM.

Therefore, for satellite radiance, let T_b be the brightness temperature, T_z is the sea water temperature of a surface channel with skin-depth z, the derivative is $\frac{\partial T_b}{\partial T_f} = \frac{\partial T_b}{\partial T_f} = (\frac{\partial T_b}{\partial T_z})(\frac{\partial T_z}{\partial T_f})$. This means that the Jacobian for radiance is provided by both RTM with available $\frac{\partial T_b}{\partial T_z}$ and NSSTM with derived $\frac{\partial T_z}{\partial T_f}$

.

The determination of the wavelength dependent skin-depth will be discussed in section 3.

2.3.1 The sensitivity of temperature at a depth to the foundation temperature: $\frac{\partial T_z}{\partial T_f}$

Let T_s be the sea water temperature required to calculate the heat fluxes at the interface, which is the SST, i.e., $T(z=0)$.

$$T_z = T_f + T'_w(z) - T'_c(z)$$

$$F(T_z, T_f) = T_z - T_f - T'_w(z) + T'_c(z) = 0$$

Using the rule of the derivative of an implicit function and the compound derivative,

$$\frac{\partial T_z}{\partial T_f} = -\frac{F'_{T_f}(T_z,T_f)}{F'_{T_z}(T_z,T_f)} = [1 - \frac{\partial T'_w(z)}{\partial T_s}\frac{\partial T_s}{\partial T_f} + \frac{\partial T'_c(z)}{\partial T_s}\frac{\partial T_s}{\partial T_f}]^{-1} \quad (27)$$

From $F(T_s, T_f) = T_s - T_f - T'_w(0) + T'_c(0) = 0$

$$\frac{\partial T_s}{\partial T_f} = -\frac{F'_{T_f}(T_s,T_f)}{F'_{T_s}(T_s,T_f)} = (1 - \frac{\partial T'_w(0)}{\partial T_s} + \frac{\partial T'_c(0)}{\partial T_s})^{-1}$$

Apply $\frac{\partial}{\partial T_s}$ to $T'_w(z) = T'_w(0) - \frac{z}{z_w}T'_w(0)$, it gives

$$\frac{\partial T'_w(z)}{\partial T_s} = \frac{\partial T'_w(0)}{\partial T_s} + \frac{1}{z_w}[\frac{T'_w(0)}{z_w}\frac{\partial z_w}{\partial T_s} - \frac{\partial T'_w(0)}{\partial T_s}]z$$

Apply $\frac{\partial}{\partial T_s}$ to $T'_c(z) = T'_c(0) - \frac{z}{\delta_c}T'_c(0)$, gives

$$\frac{\partial T'_c(z)}{\partial T_s} = \frac{\partial T'_c(0)}{\partial T_s} + \frac{1}{\delta_c}[\frac{T'_c(0)}{z_c}\frac{\partial \delta_c}{\partial T_s} - \frac{\partial T'_c(0)}{\partial T_s}]z$$

Apply $\frac{\partial}{\partial T_s}$ to $T'_w(0) = \frac{2C_t}{z_w}$, gives

$$\frac{\partial T'_w(0)}{\partial T_s} = \frac{2}{z_w}\frac{\partial C_t}{\partial T_s} - \frac{2C_t}{z_w^2}\frac{\partial z_w}{\partial T_s},$$

Let,

$$W_0 = \frac{2}{z_w}\frac{\partial C_t}{\partial T_s} - \frac{2C_t}{z_w^2}\frac{\partial z_w}{\partial T_s},\ W_d = \frac{T'_w(0)}{z_w^2}\frac{\partial z_w}{\partial T_s} - \frac{1}{z_w}\frac{T'_w(0}{\partial T_s}$$

$C_0 = \frac{1}{\kappa}[\delta_c \frac{\partial Q}{\partial T_s} + (Q - S_c - I_0 A_c \delta_c)\frac{\partial \delta_c}{\partial T_s}]$, $C_d = \frac{1}{\kappa}(I_0 A_c \frac{\partial \delta_c}{\partial T_s} - \frac{\partial Q}{\partial T_s})$

$\frac{\partial \delta_c}{\partial T_s} = (\frac{\partial Q}{\partial T_s} + C_3 \frac{\partial H_l}{\partial T_s})/(I_0 A_c - \frac{4C_1^3 \kappa^3 H_b^{1/4}}{C_2^{3/4} \delta_c^4})$, $A_c = \frac{\partial f_c}{\partial \delta_c} = a_2 - \frac{a_3}{a_4 \delta_c}(1 - e^{-\frac{\delta_c}{a_4}}) + (\frac{a_3}{\delta_c^2})(1 - e^{-\frac{\delta_c}{a_4}})$

W_0, W_d, C_0 *and* W_d are the basic variables or coefficients to calculate $\frac{\partial T_z}{\partial T_f}$ at an depth *z* in the DTL and TSL.

Therefore,

$$\frac{\partial T_w'(z)}{\partial T_s} = W_0 + W_d z \tag{28}$$

$$\frac{\partial T_c'(z)}{\partial T_s} = C_0 + C_d z \tag{29}$$

$$\frac{\partial T_s}{\partial T_f} = (1 - \frac{\partial T_w'(0)}{\partial T_s} + \frac{\partial T_c'(0)}{\partial T_s})^{-1} = \frac{1}{1 - W_0 + C_0} \tag{30}$$

Substitute (20), (21), and (22) into (19),

$$\frac{\partial T_z}{\partial T_f} = \frac{1 - W_0 + C_0}{1 - 2W_0 + 2C_0 - W_d z + C_d z} \tag{31}$$

The final or actual $\frac{\partial T_z}{\partial T_f}$ is situation dependent. $\frac{\partial T_z}{\partial T_f} = 1$ by default.

When both DTL and TSL exist, $T_w'(0) > 0$ and $T_c'(0) > 0$:

$\frac{\partial T_z}{\partial T_f} = \frac{1 - W_0 + C_0}{1 - 2W_0 + 2C_0 - W_d z + C_d z}$, $0 < z \le \delta_c$

$\frac{\partial T_z}{\partial T_f} = \frac{1 - W_0 + C_0}{1 - 2W_0 + 2C_0 - W_d z}$, $\delta_c < z \le z_w$

When TSL exists but no DTL, $T_w'(0) = 0$ and $T_c'(0) > 0$,

$\frac{\partial T_z}{\partial T_f} = \frac{1 + C_0}{1 + 2C_0 + C_d z}$, $0 < z \le \delta_c$

2.3.2 The evolution equations of $\frac{\partial z_w}{\partial T_s}$ and $\frac{\partial C_t}{\partial T_s}$

Both DTL and TSL make contribution to $\frac{\partial T_z}{\partial T_f}$, the TSL is resolved by a parameterization scheme, but DTL is by 5 ordinary diffirentcial equations. All the variables or parameters required can be obtained at any time with the known fluxes and solar penetration parameterization. For DTL part, it can be seen that two variables, $\frac{\partial z_w}{\partial T_s}$ and $\frac{\partial C_t}{\partial T_s}$, are primary. They vary with the time and there is no available formula to get them. Here, the solution is to derive their evolution equations and add to the DTL control equations and then solve them together (8) to (12) as a single system.

Apply $\frac{\partial}{\partial T_s}$ to (8) and (12), gives,

$$\frac{\partial}{\partial t}\left(\frac{\partial C_t}{\partial T_s}\right) = \frac{1}{\rho_0 c_p}\left(I_0 A_w \frac{\partial z_w}{\partial T_s} - \frac{\partial Q}{\partial T_s}\right) \tag{32}$$

$$\frac{\partial}{\partial t}\left(\frac{\partial z_w}{\partial T_s}\right) = \frac{1}{C_u^2 + C_v^2}\left(A z_w^3 + B\frac{\partial z_w}{\partial T_s}\right) \tag{33}$$

$$A = \frac{1}{4R_{ic}\rho_0}\left(\frac{\alpha}{c_p}\frac{\partial Q}{\partial T_s} + \frac{\beta S_r}{L_v}\frac{\partial E}{\partial T_s}\right)$$

$$B = \frac{\tau_x C_u + \tau_y C_v}{\rho_0} - \frac{\alpha g I_0 f_w' z_w^3}{4R_{ic} c_p \rho_0} + \frac{3g\Delta\rho z_w^2}{4R_{ic}}$$

2.3.3 The initial condition determination of $\frac{\partial z_w}{\partial T_s}$ and $\frac{\partial C_t}{\partial T_s}$

From section 2.2.3, When $f \approx 0$ $(-1^\circ < latitude < 1^\circ)$, then,

$$z_w = (2R_{ic}\Delta t/\rho_0)^{1/2}\tau / \{(\alpha g/c_p)[f_w(z_w)I_0 - Q] - \beta g \rho_0 S_r (E - P)\}^{1/2}$$

Write in the implicit function,

$$F(z_w, T_s) = \{(\frac{\alpha g}{c_p})[f_w(z_w)I_0 - Q] - \beta g \rho_0 S_r [E(T_s) - P]\} z_w^2 - \frac{2R_{ic}\Delta t \tau^2}{\rho_0} = 0 \tag{34}$$

Therefore,

$$\frac{\partial z_w}{\partial T_s} = -\frac{F'_{T_s}(z_w, T_s)}{F'_{z_w}(z_w, T_s)} = \frac{(\frac{\partial Q}{\partial T_s})z_w + (\frac{\rho_0 c_p \beta S_r}{\alpha})(\frac{\partial E}{\partial T_s})z_w}{I_0 A_w z_w + 2[f_w(z_w)I_0 - Q] - 2(\frac{\rho_0 c_p \beta S_r}{\alpha})(E - P)} \tag{35}$$

Note the same $\frac{\partial z_w}{\partial T_s}$ is the same when $f > 0$, since the derivative of the last term in (12) is zero.

Integrate (8) one step with the initial z_w in 2.2.3, gives

$$C_t = \frac{\Delta t[f_w(z_w)I_0 - Q]}{(\rho_0 c_p)} \tag{36}$$

Apply $\frac{\partial}{\partial T_s}$ to (14), therefore, the initial condition of $\frac{\partial C_t}{\partial T_s}$ is

$$\frac{\partial C_t}{\partial T_s} = \frac{\Delta t}{\rho_0 c_p}\left(I_0 A_w \frac{\partial z_w}{\partial T_s} - \frac{\partial Q}{\partial T_s}\right) \tag{37}$$

3. **Analysis scheme**

A surface temperature analysis variable has added to NCEP data assimilation system since it is switched from SSI in GSI (Derber et al, 1991). This analysis is done but not used in GFS yet.

3.1 Observations

The observations used in this study include all the observations available in NCEP atmospheric analysis, including HIRS, AIRS, IASI, GOES sounder, AMSUA, AMSUB, SSMI, plus the newly introduced AVHRR GAC radiance, AMSRE radiance and in situ sea temperature observations.

The depth of the buoys and ships is determined by inventories and contacts to the related data centers. For the fixed buoys, the depth can be 0.6, 1.0, 1.2 or 1.5 meters. For drifting buoys, there is buoy specific depth information available, and it is know it in the range of 0.20 to 0.45 meters. The 0.25 m is used for all the drifting buoys here. For ships, the depths, in the range of about 1.0 m to 10+ m, are determined with a table from Volunteer Observation Ships (VOS), but not available to all the ships. For the buoys and ships without any depth information, the depth is assigned as 1 m.

Ideally, the satellite radiance skin-depth is calculated by a model. Here, it is handled in a simple way. For all Infra-Red channels, it is assigned as $15\ \mu m$. For Microwave channels, it is assigned as $30\ mm$ for AMERE, and $1\ mm$ for the rest.

3.2 The analysis variable selection

The NSST-Profile, $T(z)$, can split into three components, the foundation temperature, DTL profile and TSL profile, $T(z) = T_f(z_w) + T'_w(z) - T'_c(z)$. Define the SST to be the temperature at $SST = T(0)$, then, $SST = T(0) = T_f + T'_w(0) - T'_c(0)$. Note $T'_w(z)$ is valid when $z \le z_w$ and $T'_c(0)$ is valid when $z \le \delta_c$.

As discussed in introduction and section 2.3, the work is done here in the frame of the whole profile, instead of the temperature at a depth. The profile has been simulated by NSSTM, ideally, it should be analyzed as well. However, it is too expensive in this project even under the linear profile assumption to analyze the profile. The strategy here is to analyze only one temperature at a specific depth, the profile is simulated by the model.

Here, the T_f is analyzed, $T'_w(z)$ and $T'_c(z)$ are simulated by NSSTM. In principle, any temperature on the NSST-Profile can be the analysis variable with the direct assimilation concept, including the one which is never observed directly such as SST. The reasons to select T_f as the analysis variable: (1) The slower varying T_f than other candidates, such as SST (at surface) and skin temperature (at IR skin-depth), has smaller analysis increment. This is helpful particularly no T_f forward model yet. (2) It physically represents the mixed layer temperature just as the bulk temperature has been used in the previous SST analysis. Therefore, the new analysis can start from what have been developed in available NCEP SST analysis such as background covariance.

3.3 Analyze SST within the NCEP GFS

The surface temperature, as an analysis variable, was added to GSI and analyzed together with the atmospheric analysis variables some years ago (Parrish et al, 1991; Derber et al, 1998?). Before the NSST profile concept is introduced as here, over ocean, the analysis variable is actually defined bulk temperature, the same as in the independent SST or bulk temperature analysis, which is used as the thermal lower boundary condition in radiance simulation. Obviously, the inconsistency between the

analysis variable (depth independent) and the observations (depth dependent) leads to analysis error. More importantly, this surface temperature analysis is never evaluated and not used in the GFS cycling.

Here, the SST, with the foundation temperature as the analysis variable, newly introduced AVHRR GAC radiance, AMSRE radaince and in situ sea water temperature observations, is analyzed together with the atmospheric analysis variables within the NCEP GFS 6-hourly. All the observations, including satellite and in situ data, are assimilated directly by the variational assimilation technique of GSI.

The background error variance and correlation length are the same as those in RTG SST analysis. The satellite radiance bias correction and thinning, quality control follows GSI.

The Community Radiative Transfer Model (CRTM) is used in NCEP GFS. The water surface temperature, $SST_z^{crtm} = T_f + T'_w(z) - T'_c(z)$, provided to CRTM is skin-depth dependent.

4 Experiments and validation

4.1 Experiments

Two cycling runs, CTL and EXP, have been performed with NCEP GFS 2011 version at T574 resolution for two periods of May 12, 2010 to September 30, 2010 and November 12, 2010 to February 28, 2011. The only difference between CTL and EXP is the SST in analysis and prediction. In CTL, weekly Reynolds SST is used as the lower boundary condition of CRTM and atmospheric model. In CTL, foundation temperature is analyzed with GSI, the T-Profile is simulated by NSSTM. The skin-depth dependent lower thermal boundary condition is provided to CRTM. The high frequency SST variability due to DTL and TSL is included in the prediction mode. A 16-day forecasting starting from 00Z is performed for both summer and winter seasons. And the 16-day predictions from 00Z, 06Z, 12Z and 18Z are done for January 2011.

4.2 Validation

Figure 3. Histogram of O-B against drifting buoys sea water temperature observations. for CTL and EXP, Global.

4.2.1 O-B & O-F against drifting buoy observations

4.2.2 SST bias and rms against own analysis

4.2.3 Weather forecasting

5 Conclusions

Appendix I **Partial derivative of heat fluxes to sea surface temperature (** T_s)

$\frac{\partial R_{nl}(T_s)}{\partial T_s}$, $\frac{\partial H_s(T_s)}{\partial T_s}$ *and* $\frac{\partial H_l(T_s)}{\partial T_s}$ can be calculated with their parameterization formula.

Net upward long wave radiation flux and its sensitivity to T_s **:**

$R_{nl} = \epsilon\sigma T_s^4 - R_{dl}$, $\sigma = 5.673\times10^{-8}$ is Stefan-Boltzmann Constant, ϵ is the emissivity of the sea water, R_{dl} is the downward longwave radiation.

$\frac{\partial R_{nl}}{\partial T_s} = 4\epsilon\sigma T_s^3$

Sensible Heat flux and its sensitivity to T_s **:**

$H_s = \rho_a c_p C_H V_a (\frac{P_0}{P_s})^{\frac{R_d}{c_p}} (T_s - T_a)$

C_H: sensible heat exchange coefficient. $V_a = (u^2 + v^2 + w_g^2)^{1/2}$ u, v are the zonal and meridional components of the surface wind, w_g is the convective gustiness.

$\frac{\partial H_s}{\partial T_s} = \rho_a c_p C_H V_a (\frac{P_0}{P_s})^{\frac{R_d}{c_p}}$

Rainfall sensible Heat flux and its sensitivity to T_s **:**

Latent Heat flux and its sensitivity to T_s **:**

After saturation vapor pressure is calculated, the saturation humidity, latent heat flux and the sensitivity of latent heat flux to sea skin temperature can be obtained:

$H_l = \rho_a L C_E V_a (q_s - q_a)$, C_E : latent heat exchange coefficient.

$q_s = \frac{0.622 e_s}{P_s - 0.378 e_s}$

$\frac{\partial H_l}{\partial T_s} = \rho_a L C_E V_a \frac{0.622 P_s}{(P_s - 0.378 e_s)^2} \frac{\partial e_s}{\partial T_s}$

When $T_s \geq 273.16$:

$$e_{s\_liq}(T_s) = C_{psat}(\frac{273.16}{T_s})^{\frac{(C_{liq}-C_{vap})}{R_\upsilon}} exp[(\frac{C_{liq}-C_{vap}}{R_\upsilon} + \frac{L_c}{273.16R_\upsilon})(1 - \frac{273.16}{T_s})]$$

Here, C_{psat} is pressure at water 3-phase point. L_c is water vapor condensation latent heat. C_{liq} is specific heat of liquid water. C_{vap} is specific heat of water vapor. L_c is water vapor condensation latent heat. L_f is water vapor fusion latent heat.

Let $a_{liq} = \frac{(C_{liq}-C_{vap})}{R_\upsilon} = 5.286$, $b_{liq} = \frac{(C_{liq}-C_{vap})}{R_\upsilon} + \frac{L_c}{(273.16R_\upsilon)} = 25.12$

Then,

$$e_{s\_liq}(T_s) = 610.78(\frac{273.16}{T_s})^{a_{liq}} exp[b_{liq}(1 - \frac{273.16}{T_s})]$$

Therefore, $\frac{\partial e_{s\_liq}}{\partial T_s = \frac{(273.16 b_{liq} - a_{liq} T_s) e_{s\_liq}}{T_s^2}}$

When $T_s \leq 253.16$,

$$e_{s\_sol}(T_s) = C_{psat}(\frac{273.16}{T_s})^{\frac{(C_{sol}-C_{vap})}{R_\upsilon}} exp[(\frac{C_{sol}-C_{vap}}{R_\upsilon} + \frac{L_i}{273.16R_\upsilon})(1 - \frac{273.16}{T_s})]$$

Here, C_{sol} is specific heat of solid water (ice). $L_i = L_f + L_c$.

Let $a_{sol} = \frac{(C_{sol}-C_{vap})}{R_\upsilon} = 0.5634$, $b_{sol} = \frac{(C_{sol}-C_{vap})}{R_\upsilon} + \frac{L_i}{(273.16R_\upsilon)} = 23.04$, then

$$e_{s\_sol}(T_s) = 610.78(\frac{273.16}{T_s})^{a_{sol}} exp[b_{sol}(1 - \frac{273.16}{T_s})]$$

$$\frac{\partial e_{s\_sol}}{\partial T_s = \frac{(273.16 b_{sol} - a_{sol} T_s) e_{s\_sol}}{T_s^2}}$$

When $253.16 \leq T_s \leq 273.16$, then,

$$e_{s\_mix}(T_s) = w e_{s\_liq}(T_s) + (1 - w) e_{s\_sol}(T_s),$$

Here, $w = \frac{(T_s - 253.16)}{20}$ and therefore $\frac{\partial w}{\partial T_s = \frac{1}{20}}$,

$$\frac{\partial e_{s\_mix}}{\partial T_s = w} \frac{\partial e_{s\_liq}}{\partial T_s + (1-w)\frac{\partial e_{s\_sol}}{\partial} T_s} + \frac{(e_{s\_liq} - e_{s\_sol})}{20}$$

References

Dalu GA, Purini R. 1981. The diurnal thermocline due to buoyant convection. Q. J. R. Meteorol. Soc. **108**: 929-935.

Donlon CJ, Robinson I, Casey K, Vasquez J, Armstrong E, Gentemann C, May D, LeBorgne P, Piollé J, Barton I, Beggs H, Poulter DJS, Merchant C, Bingham A, Heinz S, Harris A, Wick G, Emery B, Stuart-Menteth A, Minnett P, Evans B, Llewellyn-Jones D, Mutlow C, Reynolds R, Kawamura H, & Rayner N. 2007. The GODAE high resolution sea surface temperature pilot project (GHRSST-PP). Bulletin of American Meteorological Society, **88**: 1197–1213.

Donlon CJ, Martin M, Stark J, Roberts-Jones J, Fiedler E, Wimmer W. 2012. The operational sea surface temperature and sea ice analysis (OSTIA) system. Remote Sensing of Environment. **116**: 140-158.

Fairall CW, Bradley EF, Godfrey JS, Wick GA, Edson JB, and Young GS. 1996. Cool-skin and warm-layer effects on sea surface temperature. J. Geophys., Res. **101**: 1295-1308.

Gentemann CL, Minnett PJ, Borgne PL, and Merchant CJ. 2008. Multi-satellite measurements of large diurnal warming events. Geophysical Research Letters. Vol. 35, Issue 22.

Gentemann CL, Minnett PJ, Ward B. 2009. Profiles of ocean surface heating (POSH): A new model of upper ocean diurnal warming. J. Geophys., Res. **114**, C07107. doi: 10. 1029/2008GC004825, 2009.

Niiler PP, and Kraus EB. 1977. One-dimensional models, in Modeling and Prediction of the Upper Layers of the Ocean, edited by E.B. Kraus, pp. 143-172, Pergamon, New York.

Parrish, D.F.,and J.C. Derber, 1992: The National Meteorological Center's spectral statistical-interpolation system. Mon. Wea. Rev., **120,** 1747–1763.

Paulson TN and Simpson JJ. 1981: The temperature difference across the cool skin of the ocean. J. Geophys., Res., **86(C11):** 11044 – 11055.

Phillips O.M., 1977: The Dynamics of the Upper Ocean. 336 pp. Cambridge Press, New York.

Price JF, Weller RA, and Pinkle R. 1986: Diurnal cycling: *Observations* and models of the upper ocean response to diurnal heating, cooling, and wind mixing. J. Geophys. Res., **91**: 8411-8427.

Reynolds RW, Smith T. 1994. Improved global sea surface temperature analysis using optimum interpolation. J. Climate, Vol. 7, Issue **6**: 929-948.

Robinson IS. 2004. Measuring the Oceans from Space: The principles and methods of satellite oceanography. Springer Praxis Publishing. Chichester, UK.

Thiébaux J., Rogers E., Wang W., and Katz B. 2003: A new high-resolution blended real-time global sea surface temperature analysis. *Bull. Amer. Meteor. Soc.,* **84,** 645–656.

Webster PJ, Clayson CA and Curry JA. 1996. Clouds, radiation and the diurnal cycle of sea surface temperature in the tropical western Pacific Ocean. J. Climate, **9**: 1712-1730.

Zeng X., Beljasrs A. 2005: A prognostic scheme of sea surface skin temperature for modeling and data assimilation. Geophysical Research Letters, Vol. 32, L14605. doi: 10. 1029/2005GL023030, 2005.

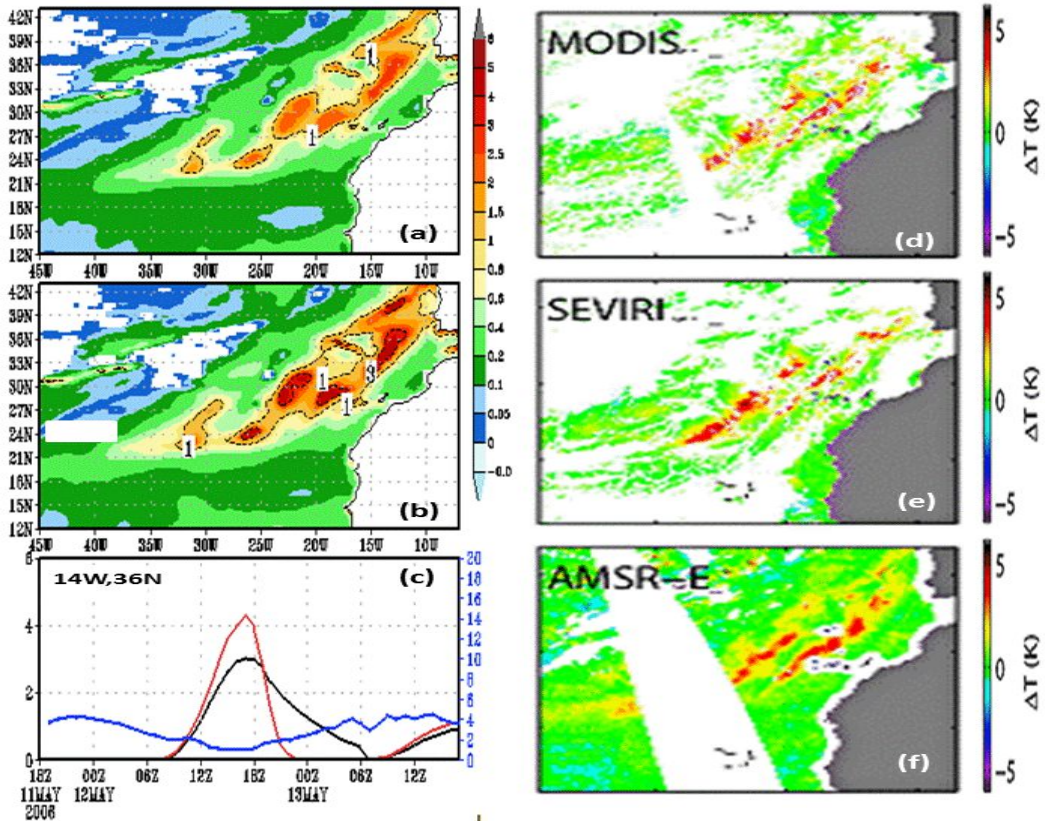

Figure 2. The diurnal warming amount simulated by diurnal thermocline model and estimated by satellite SST retrieval in the area of (45W – 5W, 12N – 43 N) at 14Z, May12, 2006: (a) NCEP dtm-1p; (b) COARE V3.0. (d) MODIS retrieval. (e) SEVIRI retrieval. (f) AMSR-E retrieval. (c) Time series of diurnal warming and wind at the location of (14W, 36N).

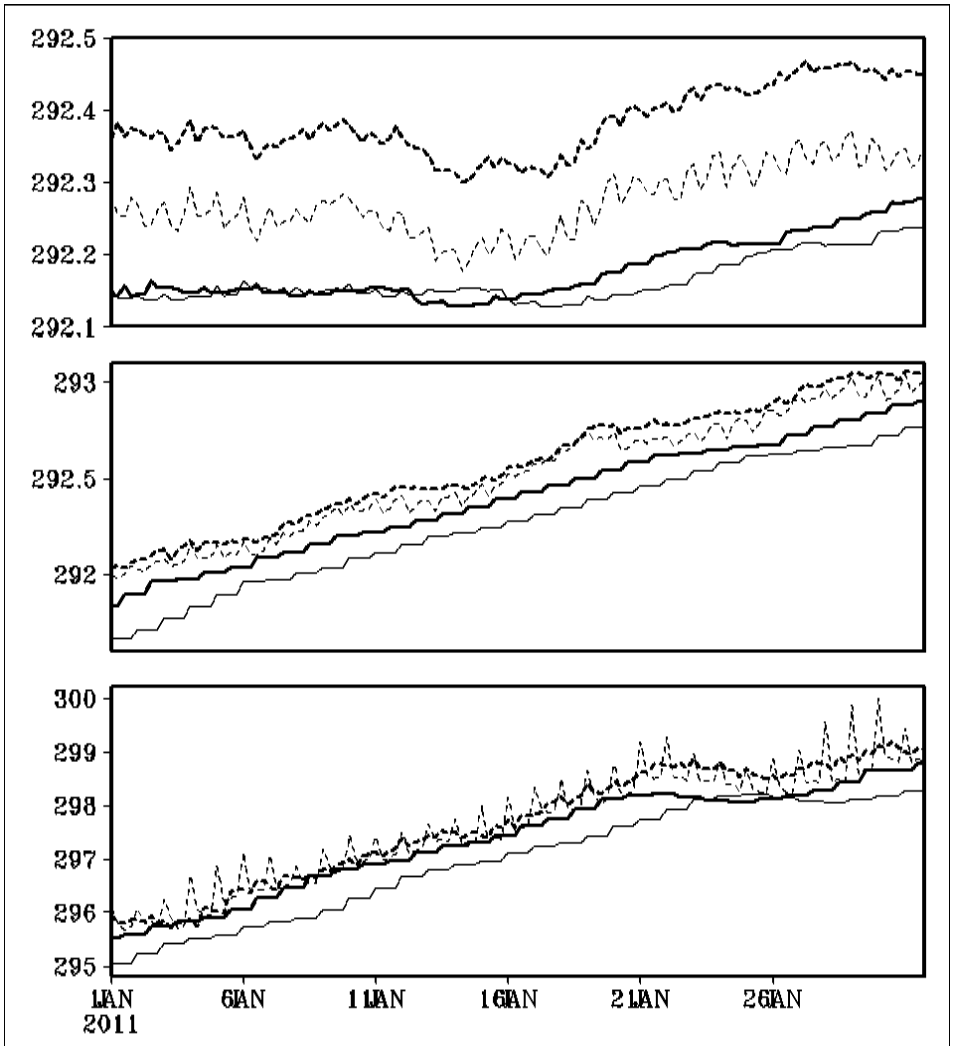

Figure 3. Time series of oceanic temperature analysis for January 2011. (a) Global; (b) Southern Mid-latitude (20 S – 50 S). (c) A 20 by 10 degree area in South Pacific ocean (170 W – 150 W, 25 S – 35 S). Thin solid line: CTL SST; Thin dashed line: EXP SST. Thick dashed line: Tf; Thick solid line, CTL SST but shifted three and half day ahead.

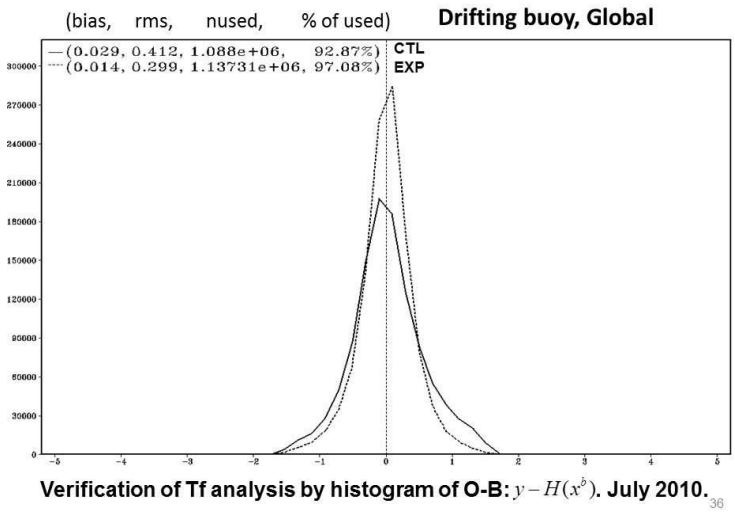

Figure 4. Histogram of O-B against drifting buoys sea water temperature observations. for CTL and EXP, Global.

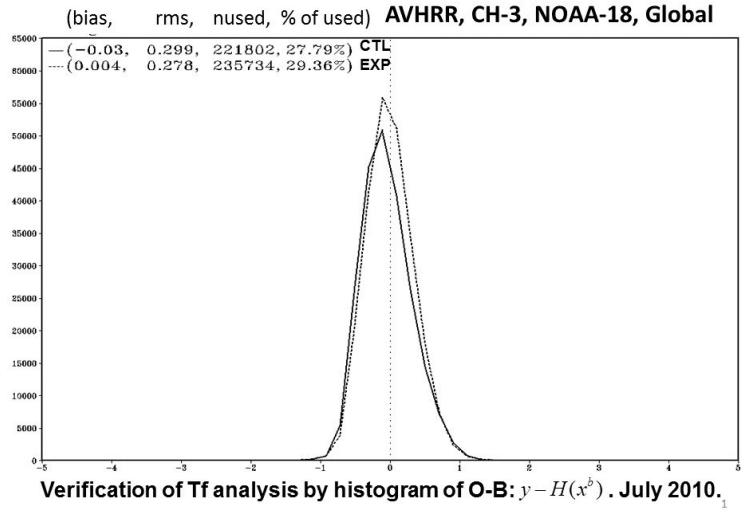

Figure 5. Histogram of O-B of NOAA-18 AVHRR channel-3 radiance for CTL and EXP, July, 2010 . Global.

Area	Run	Analysis	Day 1	Day 3	Day 5	Day 7	Used data
N.Pole (50N – 90N)	EXP	0.003, 0.276	-0.00, 0.339	-0.01, 0.419	-0.03, 0.467	-0.05, 0.515	90777 (97.19%)
	CTL	0.105, 0.537	0.099, 0.541	0.131, 0.554	0.168, 0.567	0.190, 0.589	86909 (93.05%)
N.Mid (20N – 50N)	EXP	0.01, 0.332	-0.04, 0.378	-0.10, 0.446	-0.17, 0.507	-0.23, 0.563	333920 (93.61%)
	CTL	-0.12, 0.464	-0.15, 0.481	-0.17, 0.497	-0.18, 0.514	-0.19, 0.532	324698 (91.02%)
Tropics (20S – 20N)	EXP	0.035, 0.206	0.030, 0.232	0.026, 0.279	0.023, 0.319	0.006, 0.354	257572 (98.69%)
	CTL	-0.03, 0.302	-0.03, 0.316	-0.05, 0.333	-0.06, 0.349	-0.07, 0.361	256262 (98.19%)
S.Mid (20S – 50S)	EXP	-0.01, 0.322	0.008, 0.374	0.070, 0.477	0.139, 0.559	0.212, 0.625	277374 (96.36%)
	CTL	0.098, 0.474	0.131, 0.501	0.142, 0.540	0.156, 0.573	0.173, 0.602	266842 (92.70%)
S.Pole (50S – 90S)	EXP	0.007, 0.352	0.030, 0.411	0.083, 0.500	0.134, 0.562	0.161, 0.604	61847 (97.16%)
	CTL	0.102, 0.483	0.124, 0.502	0.124, 0.525	0.120, 0.540	0.119, 0.553	60218 (94.60%)
Global	EXP	0.001, 0.294	-0.00, 0.339	-0.00, 0.413	-0.00, 0.474	-0.01, 0.526	1021440 (96.13%)
	CTL	-0.00, 0.433	-0.00, 0.451	-0.01, 0.473	-0.01, 0.494	-0.01, 0.513	994873 (93.63%)
S.Mid.Pac (170W – 150W, 25S – 35S)	EXP	0.043, 0.234	0.114, 0.306	0.314, 0.516	0.520, 0.689	0.754, 0.883	6976 (99.18%)
	CTL	0.483, 0.561	0.585, 0.657	0.748, 0.814	0.920, 0.961	1.092, 1.115	6215 (88.36%)

Table 1. The validation, based on (O – B) statistics, of the analysis and prediction of SST, January 2011. Bias and RMS are shown in each grid for analysis and the prediction of Day-1, Day-3, Day-5 and Day-7. The number and percentage of the used data are shown as well.

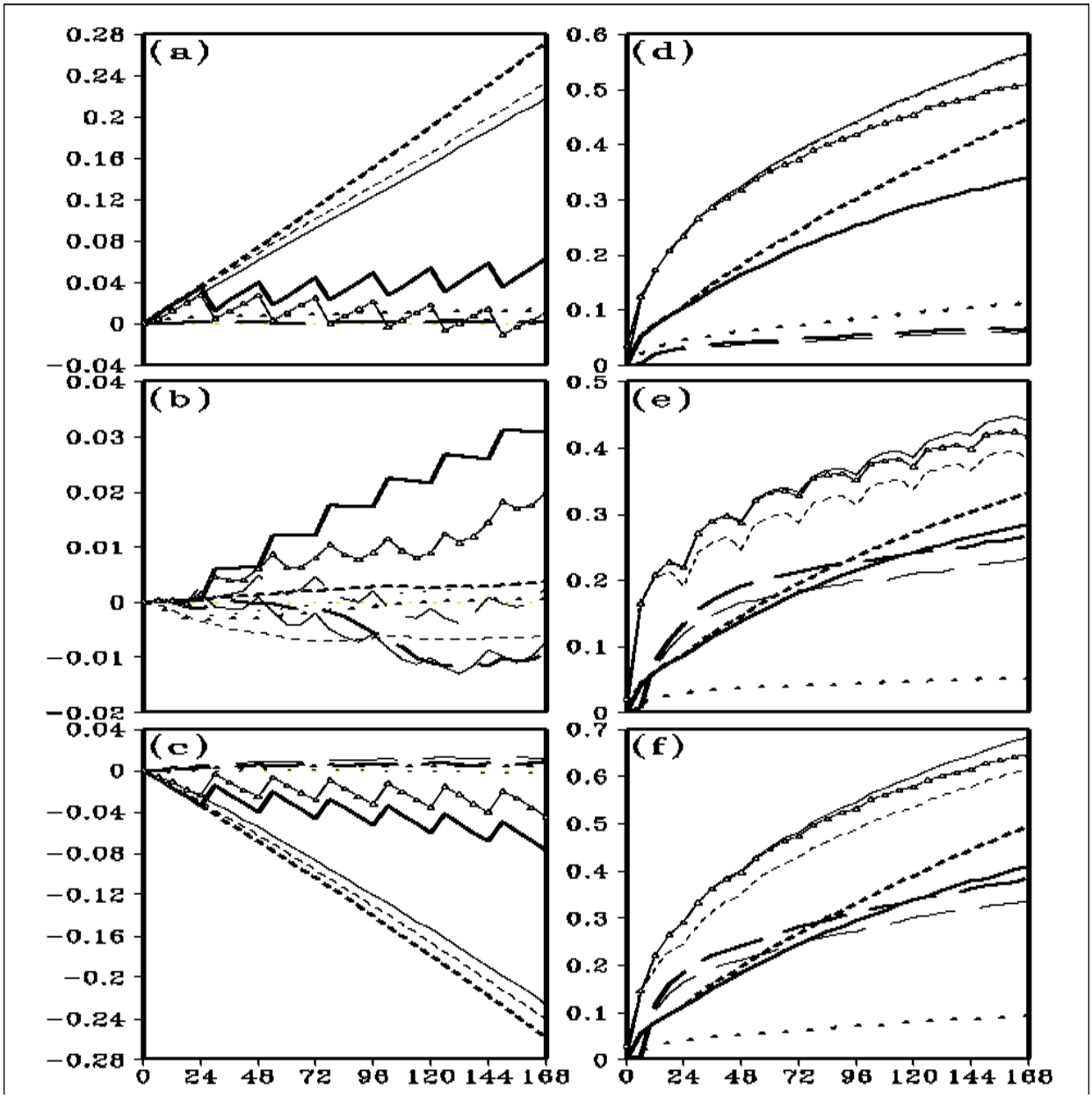

Figure 6. Prediction error of the oceanic variables for January 2011. (a) Bias of NH; (b) Bias of Tropics; (c) Bias of SH; (d) RMS of NH; (e) RMS of Tropics; (f) RMS of SH. Thick solid line: CTL SST. Thin solid line: EXP SST. Thin dashed line: EXP T_f. Thick long dashed line: CTL $T_w'(0)$(surface diurnal warming amount). Thin long dashed line: EXP $T_w'(0)$(surface diurnal warming amount). Thick dotted line: CTL $T_c'(0)$ (surface sub-layer cooling amount). Thin dotted line: EXP $T_c'(0)$ (surface sub-layer cooling amount). Thin solid line with triangle mark: EXP SST with climatology correction. Thick dashed line: CTL SST without climatology correction.

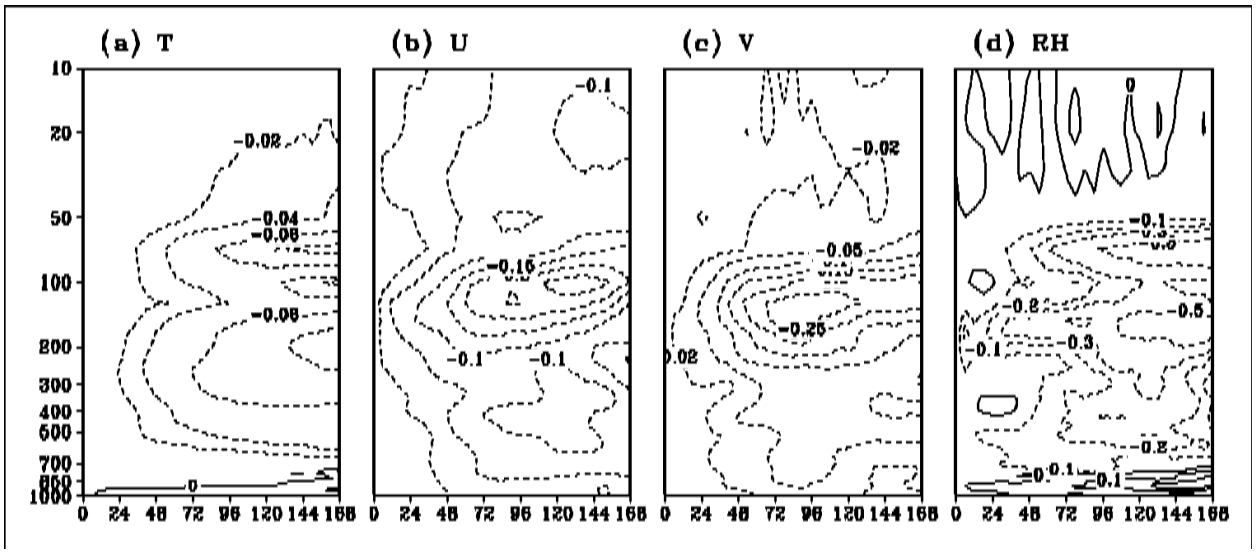

Figure 6. The predicted RMS difference between EXP and CTL for 124 7-day forecasting of January 2011 in Tropics. The verification is against the own analysis. (a) Air temperature (T). (b) Zonal wind (U). (c) Meridional wind (V). (d) Relative humidity (RH).

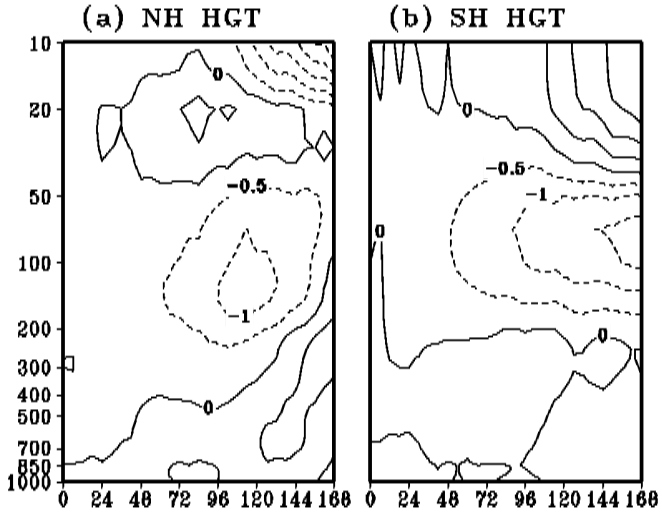

Figure 7. The predicted geopotential height RMS difference between EXP and CTL for 124 7-day forecasting of January 2011. The verification is against the own analysis. (a) NH; (b) SH.

Two new interactions are introduced and they will enhance the impact of ocean on the weather prediction. Air-sea interaction by the air-sea coupling in coupled prediction, analysis and prediction interaction by cycling, including both atmosphere and ocean, in NWP cycling.

Considering the feedback between the analysis and forecasting due to the cycling in NWP, the SST analysis becomes even more important since the impact of any variable is indispensable in the integrated system. The evolution of SST needs to be addressed not only in the forecasting step for a realistic oceanic variation, but also in the analysis for a time match radiance simulation to the observations.

Therefore, the feedback between the background and the analysis is essential for the atmosphere in NWP. However, this is not true for the oceanic component, since SST is analyzed independently and specified instead of predicted as the atmosphere in the system.